

Can the speed of sound of quark-gluon plasma be measured from the multiplicity and mean p_T of ultracentral heavy-ion collisions?

Lorenzo Gavassino,^{1,*} Henry Hirvonen,^{1,2,†} Jean-François Paquet,^{2,1,‡} Mayank Singh,^{2,§} and Gabriel Soares Rocha^{3,2,¶}

¹*Department of Mathematics, Vanderbilt University, Nashville, TN 37240, USA*

²*Department of Physics and Astronomy, Vanderbilt University, Nashville, TN 37240, USA*

³*Instituto de Física, Universidade Federal Fluminense, Niterói, Rio de Janeiro, 24210-346, Brazil*

The mean transverse momentum $\langle p_T \rangle$ of hadrons has been observed experimentally and in numerical simulations to have a power-law dependence on the hadronic multiplicity N in ultracentral relativistic heavy-ion collisions: $\langle p_T \rangle \propto N^{b_{UC}}$. It has been put forward that this exponent b_{UC} is the speed of sound of quark-gluon plasma measured at a temperature determined from $\langle p_T \rangle$. We study step by step the connection between (i) the energy and entropy of hydrodynamic simulations and (ii) experimentally measurable observables. We show that an argument based on energy and entropy should yield an exponent equal to the pressure over energy density P/ε , rather than the speed of sound c_s^2 ; however, we also observe that $\langle p_T \rangle$ and N are not sufficiently accurate proxies for the energy and entropy to make this possible in practice. From simulations, we find that the exponent b_{UC} is significantly different whether the “effective volume” is strictly constant or not, a condition that cannot be enforced experimentally. Additional tests using a modified equation of state find that the exponent b_{UC} exhibits a variable degree of correlations with the speed of sound and with P/ε , but is not an accurate measurement of either quantity in general.

I. INTRODUCTION

Ultrarelativistic heavy-ion collision experiments at the Large Hadron Collider (LHC) access the high-temperature, low-baryon chemical potential regime of the quantum chromodynamics (QCD) phase diagram [1–5]. Thermodynamic properties of bulk QCD matter produced in these collisions are related to each other by the equation of state. The QCD equation of state has been computed from first principles using lattice QCD techniques [6–9]. It has also been studied from measurements using Bayesian inference [10].

Recently, it was claimed that the QCD equation of state can be directly inferred from experiments in ultracentral collisions [11–13]. More specifically, the speed of sound squared (c_s^2) at an effective temperature, T_{eff} , was equated to the experimental observable

$$b_{UC} \equiv \frac{d \ln \langle p_{T,\text{ch}} \rangle}{d \ln N_{\text{ch}}}, \quad (1)$$

for ultracentral events. Here, $\langle p_{T,\text{ch}} \rangle$ is the mean transverse momentum of the particles and N_{ch} is their multiplicity. This observable has been measured by the CMS [14], ATLAS [15] and ALICE [16] collaborations and compared to lattice QCD calculations [17]. Studying ultracentral Pb-Pb collisions at $\sqrt{s_{NN}} = 5.02$ TeV, the CMS Collaboration found an excellent agreement of b_{UC} with the lattice result for the speed of sound; on the other

hand, the ALICE Collaboration observed a large dependence of b_{UC} on the method used for centrality determination. The latter effects were also studied in numerical simulations [18].

The purpose of this work is to study the validity and generality of the claim $b_{UC} \stackrel{?}{=} c_s^2$ in various situations. This paper is organized in the following way. In Sec. II we go through the original argument and discuss the theoretical difficulties in connecting b_{UC} with the thermodynamic properties of the plasma. The framework that we use to systematically study the observable b_{UC} is introduced in Sec. III. The main results of our work are presented in Sec. IV, and final conclusions of our work are given in Sec. V.

II. CONNECTING b_{UC} TO QCD THERMODYNAMICS

In thermodynamics, the speed of sound squared at zero baryon density is defined as $c_s^2 \equiv dP/d\varepsilon = d \ln T / d \ln s$, where P is pressure, ε is the energy density, T is temperature and s is entropy density. Quark-gluon plasma is not in global thermodynamic equilibrium, but one can define effective thermodynamic variables — an effective temperature T_{eff} and an effective volume V_{eff} — through the equalities

$$\begin{aligned} E &\equiv \varepsilon(T_{\text{eff}})V_{\text{eff}}, \\ S &\equiv s(T_{\text{eff}})V_{\text{eff}}, \end{aligned} \quad (2)$$

where E and S are the total energy and total entropy on a constant-temperature hypersurface that encloses a certain spacetime region of the plasma. Because this hypersurface is generally taken to enclose a finite region in

* lorenzo.gavassino@vanderbilt.edu

† henry.v.hirvonen@vanderbilt.edu

‡ jean-francois.paquet@vanderbilt.edu

§ mayank.singh@vanderbilt.edu

¶ gabriel.soares.rocha@vanderbilt.edu

spatial rapidity, E and S represent only part of the energy and entropy of the plasma. In particular, they are *not* conserved quantities — energy and entropy flow in the longitudinal direction — but they are well defined in numerical simulations.

Two key assumptions are that (i) the medium is in local thermal equilibrium on this hypersurface, and that (ii) the energy E and entropy S on this hypersurface are closely related to the energy and multiplicity of particles measured at the end of the collision.

A. Speed of sound vs. P/ε

The original argument for the equivalence between b_{UC} and c_s^2 made in Refs. [11–13] was the following. Guided by the ideal gas example and observations from numerical simulations, Refs. [11, 12] state that $\langle p_T \rangle$ is approximately proportional to the effective temperature T_{eff} [19] defined in Eq. (2). Moreover, the particle multiplicity is known to be approximately proportional to the total entropy in the system, so that $N_{\text{ch}} \propto S = s(T_{\text{eff}})V_{\text{eff}}$. If, moreover, the effective volume V_{eff} is a constant, then $N_{\text{ch}} \propto s(T_{\text{eff}})$ and one finds

$$b_{\text{UC}} \equiv \frac{d \ln \langle p_T \rangle}{d \ln N_{\text{ch}}} \underset{\substack{\langle p_T \rangle \propto T_{\text{eff}} \\ dV_{\text{eff}}=0 \\ N_{\text{ch}} \propto S}}{=} \frac{d \ln T_{\text{eff}}}{d \ln s(T_{\text{eff}})} = c_s^2(T_{\text{eff}}) \quad (3)$$

In summary, while the last equality is just a thermodynamic relation, the central equality is only valid if the following assumptions hold

- The charged hadron multiplicity N_{ch} is proportional to the hypersurface entropy S ($N_{\text{ch}} \propto S$);
- $\langle p_T \rangle \propto T_{\text{eff}}$;
- The effective volume V_{eff} is constant across different ultracentral events.

Moving beyond the original argument, we point out that a slightly different argument will yield a different interpretation for b_{UC} . There is no simple analytic expression that connects $\langle p_T \rangle$ with the hypersurface quantities, even in highly symmetric systems [20]. One case where general arguments can be made is to focus on ultrarelativistic particles at mid-rapidity, where the transverse momentum is the same as the energy, and particle multiplicity is proportional to total entropy. In this specific case, one can therefore argue that $\langle p_T \rangle \propto E/S$. If we assume that the effective volume V_{eff} is constant, then by definition $E/S = \varepsilon(T_{\text{eff}})/s(T_{\text{eff}})$, so the estimate $\langle p_T \rangle \propto E/S$ leads to a relation $\langle p_T \rangle \propto \varepsilon(T_{\text{eff}})/s(T_{\text{eff}})$, which yields

$$\frac{d \ln \langle p_T \rangle}{d \ln N_{\text{ch}}} \underset{\substack{\langle p_T \rangle \propto E/S \\ dV_{\text{eff}}=0 \\ N_{\text{ch}} \propto S}}{=} \frac{d \ln (\varepsilon(T_{\text{eff}})/s(T_{\text{eff}}))}{d \ln s(T_{\text{eff}})}. \quad (4)$$

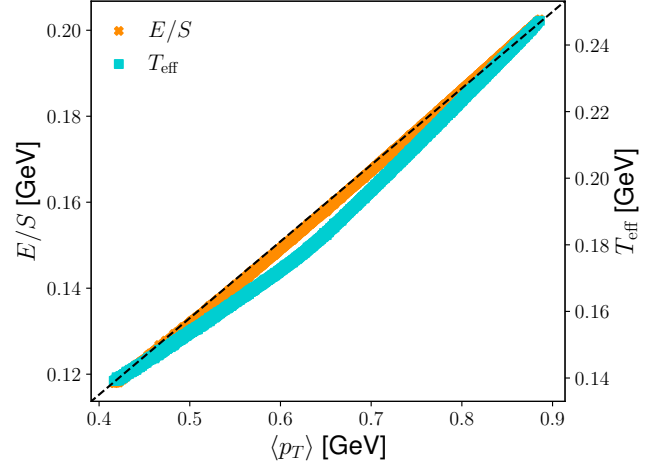


FIG. 1. The energy over entropy ratio E/S and the effective temperature T_{eff} computed on a 130 MeV constant temperature hypersurface, as a function of mean transverse momentum of charged hadrons for a QCD equation of state. The dashed black line is a straight line added as a reference.

In the absence of a chemical potential, we can write

$$\begin{aligned} \frac{d \ln (\varepsilon/s)}{d \ln s} &= \frac{d \ln \varepsilon}{d \ln s} - 1 = \frac{s}{\varepsilon} \frac{d \varepsilon}{d s} - 1 \\ &= \frac{sT}{\varepsilon} - 1 = \frac{\varepsilon + P}{\varepsilon} - 1 = \frac{P}{\varepsilon}. \end{aligned} \quad (5)$$

Hence, we have

$$b_{\text{UC}} \equiv \frac{d \ln \langle p_T \rangle}{d \ln N_{\text{ch}}} \underset{\substack{\langle p_T \rangle \propto E/S \\ dV_{\text{eff}}=0 \\ N_{\text{ch}} \propto S}}{=} \frac{d \ln (E/S)}{d \ln S} \Big|_{dV_{\text{eff}}=0} = \frac{P(T_{\text{eff}})}{\varepsilon(T_{\text{eff}})} \quad (6)$$

This is equal to c_s^2 only for special equations of state when $c_s^2 = P/\varepsilon$. Indeed, if the speed of sound is constant, the energy density is $\varepsilon = AT^{1+c_s^{-2}}$, the entropy is $s = A(1+c_s^2)T^{c_s^{-2}}$, and $\varepsilon(T_{\text{eff}})/s(T_{\text{eff}}) \propto T_{\text{eff}}$, in which case Eq. (6) reduces to Eq. (3) as expected. A study of the case with a constant speed of sound can be found in Ref. [20].

From numerical simulations, $\langle p_T \rangle$ has a strong linear correlation with both $E/S = \varepsilon(T_{\text{eff}})/s(T_{\text{eff}})$ and with T_{eff} , as shown in Figure 1. Hence, it is a priori not evident if one should expect to extract the speed of sound or the pressure over energy density ratio.

B. The effective temperature T_{eff}

For Eq. (3) or Eq. (6) to provide a measurement of the thermodynamic properties of quark-gluon plasma at given temperature, one needs the precise relation between the effective temperature T_{eff} and $\langle p_T \rangle$. In practice, the proportionality constant C in $\langle p_T \rangle = CT_{\text{eff}}$ is

determined from hydrodynamic simulations of heavy-ion collisions which use a lattice QCD based equation of state as an input. Hydrodynamic simulations use the energy and entropy on the hypersurface to calculate T_{eff} from the lattice equation of state, and take its ratio with $\langle p_T \rangle$ of charged hadrons to evaluate $C = \langle p_T \rangle / T_{\text{eff}}$. Experiments then use this coefficient to determine T_{eff} from the measured $\langle p_T \rangle$.

Previous works [11, 13] have quoted $C = 3 \pm 0.05$ based on numerical simulations for Pb-Pb collisions. On the other hand, in Ref. [21] it was found that $C \approx 2.16 - 2.8$ for p+Pb collisions. As we will discuss later in this work, we found values for $C = \langle p_T \rangle / T_{\text{eff}}$ ranging from 2.7 to 3.9, with a significant amount of variation originating from the temperature at which the hypersurface is defined.¹

C. The effective volume V_{eff}

The condition that the effective volume is constant, used in every argument, is highly non-trivial. The effective volume is not the same as the physical volume of the system. Instead, it is defined through Eq. (2). One can write an expression for V_{eff} only in terms of E and S :

$$V_{\text{eff}}(E, S) = \frac{E}{\varepsilon(s = S/V_{\text{eff}})} \quad (7)$$

where the function $\varepsilon(s)$ is defined by the underlying equation of state. This means that there is no way to have general knowledge about the effective volume without having prior information about the equation of state. As shown in Ref. [22], deviations from the constant effective volume will introduce corrections to Eqs. (3) and (6). These corrections involve derivatives $d \ln V_{\text{eff}} / d \ln S$ and thus necessarily include information from the lattice equation of state, particularly about $d \ln \varepsilon / d \ln s$.

III. MODEL DESCRIPTION

In order to test the validity of Eqs. (3) and (6) under various assumptions, we perform boost-invariant hydrodynamic simulations using the lattice QCD equation of state by HotQCD Collaboration [7]. As an initial condition for the temperature at proper time $\tau = 0.4$ fm, we use a Gaussian profile in the transverse-coordinate (x, y) plane:

$$T(\tau_0, \vec{x}_\perp) = T_0 \exp\left(-\frac{\vec{x}_\perp^2}{2\sigma^2}\right), \quad (8)$$

where τ_0 is the initial time and \vec{x}_\perp is the position in the transverse plane. The normalization of the temperature profile is set with T_0 , and σ controls the transverse width of the profile. The initial transverse velocity is set to zero. We vary T_0 across the range $[0.23, 0.67]$ GeV in increments of 0.004 GeV, while σ is varied over $[4.25, 5.06]$ fm with a step size of 0.028 fm. For each (T_0, σ) combination, we solve the ideal hydrodynamic evolution and find constant-temperature hypersurfaces [23] for various temperatures T_f using the MUSIC hydrodynamic code [24–27]. The final-state particles are obtained by sampling particles from these hypersurfaces using the Cooper-Frye procedure [28, 29] and performing decays for unstable hadrons. These are implemented using the iSS particle sampler [30]. For each hypersurface, particles are repeatedly sampled until we obtain a total of 500,000 particles at midrapidity.²

At each (T_0, σ, T_f) point, we compute the total energy E and entropy S at the hypersurface Σ as

$$\begin{aligned} E &= \int_{\Sigma} d^3\sigma_{\mu} T^{t\mu}, \\ S &= \int_{\Sigma} d^3\sigma_{\mu} s u^{\mu}, \end{aligned} \quad (9)$$

where $d^3\sigma^{\mu}$ is the directed surface element of hypersurface Σ , $T^{\mu\nu} = (\varepsilon + p)u^{\mu}u^{\nu} - Pg^{\mu\nu}$ is the energy-momentum tensor, and u^{μ} is the fluid 4-velocity. The effective temperature T_{eff} and the effective volume V_{eff} can then be computed from E and S using Eq. (2). We once again remark that, in general, solving for T_{eff} and V_{eff} requires knowing the equation of state.

Now that we know $E, S, \langle p_T \rangle, N$, and V_{eff} at every (T_0, σ, T_f) point, we construct 2D-spline interpolators in the (T_0, σ) plane for each of these at each hypersurface of constant temperature T_f . These interpolators can be used to differentiate observables with respect to T_0 and σ . To compute the variations in observables, one needs to choose how these variations arise from the initial state. In practice, for each T_f , all of our variations depend only on the initial temperature T_0 and the width σ of the initial transverse temperature profile, so for any observable \mathcal{O} , we can write:

$$d\mathcal{O} = \frac{\partial \mathcal{O}}{\partial T_0} dT_0 + \frac{\partial \mathcal{O}}{\partial \sigma} d\sigma, \quad (10)$$

and therefore we only need to choose variations dT_0 and $d\sigma$. Note that when computing quantities like $d \ln(E/S) / d \ln S$ only the ratio $d\sigma/dT_0$ matters. In the following, we use two different choices:

- The first option is to choose variations of T_0 and σ such that V_{eff} remains constant, i.e., $dV_{\text{eff}} = 0$,

¹ While it has been argued that some hypersurface temperature may be more consistent with the physics of heavy-ion collisions, we point out that the hypersurface is ultimately an artificial construct, not a physical entity: the transition from hydrodynamics to free-streaming cannot be instantaneous. Estimating $C = \langle p_T \rangle / T_{\text{eff}}$ for a fixed hypersurface temperature is bound to underestimate the uncertainty in this quantity.

² This is done because the sampling algorithm assumes a grand canonical ensemble, so the energy is not necessarily conserved in each individual sampling, but only on average.

which is consistent with the assumption made in Eqs. (3) and (6).

- The second option is to fix $d\sigma = 0$ and vary only T_0 . This approach is similar to one taken in Refs. [13, 20], but it does not guarantee that $dV_{\text{eff}} = 0$. In fact, $V_{\text{eff}} = V_{\text{eff}}(E, S)$, where E and S depend on T_0 in a non-trivial way, so that in general $(\partial V_{\text{eff}}/\partial T_0)_\sigma \neq 0$.

We note that choosing the variation along which one computes the derivatives is not unique to our model, but it also appears in more realistic event-by-event simulations. There, one needs to decide how to order the events in centrality classes before averaging over the events, and different choices can lead to different results [18].

IV. RESULTS

A. QCD equation of state

We begin by evaluating $d \ln(E/S)/d \ln S$ on hypersurfaces with three different temperatures T_f and various values of T_0 . Here we choose a reference value of $\sigma = 4.53$ fm, but we have checked that changing σ causes only minor changes. For each point, we compute T_{eff} and choose variations dT_0 and $d\sigma$ such that $dV_{\text{eff}} = 0$. In Fig. 2a), results obtained this way are compared against the speed of sound squared c_s^2 and P/ε from the HotQCD lattice equation of state [7]. Since $dV_{\text{eff}} = 0$, the last equality in Eq. (6) holds and we recover P/ε exactly, as expected.

In Fig. 2b), we show $d \ln\langle(E_{\text{ch}}/N_{\text{ch}})\rangle/d \ln N_{\text{ch}}$ evaluated from charged hadrons at midrapidity with pseudorapidity $|\eta| \leq 0.5$. In going from Fig. 2a) to 2b), we have implemented the Cooper-Frye procedure, and the appropriate kinematic cuts on the pseudorapidity of particles. This is an essential distinction from the previous step, since even for a boost invariant system at mid-rapidity, the total energy content of particles in a unit of pseudorapidity is not the same as the total energy on the hypersurface in a unit of spacetime rapidity. While the effective temperature T_{eff} is defined using the energy and entropy calculated using the spacetime-rapidity window $\eta_s \in [-0.5, 0.5]$, the observable $d \ln\langle(E_{\text{ch}}/N_{\text{ch}})\rangle/d \ln N_{\text{ch}}$ is calculated using particles with kinematic cuts on momentum pseudorapidity. Due to this reason, the results no longer agree with P/ε , but instead we get a T_f dependent shift above the P/ε curve. Importantly, the minima of $d \ln\langle(E_{\text{ch}}/N_{\text{ch}})\rangle/d \ln N_{\text{ch}}$ for the different constant-temperature hypersurfaces are observed to be closer to the minimum of P/ε than the minimum of c_s^2 .

We point out that in the late time limit, when $\tau \rightarrow \infty$ and $T_f \rightarrow 0$, the difference between the energy content on the hypersurface in a unit of spacetime-rapidity and the total energy of particles in a unit of pseudorapidity vanishes. As the hypersurface temperature is decreased, the high-momentum part of the spectrum is suppressed in the local rest frame of the fluid. In the limit $T_f \rightarrow 0$, all

the momentum of the particles come from the flow of the underlying medium. In that limit, we should recover P/ε from the observable b_{UC} . See [20] for a discussion on the late time limit of hydrodynamic evolution.³ The same pattern is also seen in Fig. 2b), where lowering the hypersurface temperature leads to a better agreement with P/ε .

Figure 2c) shows the observable b_{UC} computed from the charged hadron average transverse momentum and multiplicity — that is, in going from Fig. 2b) to c), we moved from using the mean energy of the particles to their mean transverse momentum. The latter is more easily accessible in experiments. This brings in additional corrections from the rest mass of particles in Eq. (6). We again see that there is a hypersurface temperature T_f dependence in b_{UC} and it has shifted further above the P/ε curve. However, the temperature dependence of the b_{UC} still closely resembles the shape of P/ε . Moreover, Fig. 2c) proves that in general, the statements $\langle p_T \rangle \propto T_{\text{eff}}$ and $N_{\text{ch}} \propto S$ are not both sufficiently accurate, since otherwise all points would agree with c_s^2 as per Eq. (3). If $dV_{\text{eff}} = 0$ was actually true across different ultracentral events, Fig. 2c) is the observable that we would expect to measure in experiments: a quantity correlated with P/ε and c_s^2 , but not an accurate measurement of either.

Finally, in going from Fig. 2 c) to d) we relax the requirement $dV_{\text{eff}} = 0$. This effectively means that we just vary the initial normalization T_0 in our simulations and keep the Gaussian width σ of the initial temperature profile fixed. As seen in Fig. 2d), the dependence of the observable on the temperature T_f of the hypersurface is much smaller. This appears to be an accidental cancellation of effects from kinematic cuts and V_{eff} dependence. The observable b_{UC} is again shifted above the P/ε curve and is close to c_s^2 for temperatures between 180 MeV to 230 MeV. At lower temperatures, there is a noticeable dependence on the hypersurface temperature and the observable is inconsistent with c_s^2 .

The agreement between b_{UC} and c_s^2 in the narrow temperature region appears to be a coincidental accumulation of effects from assumptions $\langle p_T \rangle \propto E/S = \varepsilon(T_{\text{eff}})/s(T_{\text{eff}})$ and $dV_{\text{eff}} = 0$ and we have no reason to believe that this is a general feature. In fact, the case with $dV_{\text{eff}} = 0$ is noticeably farther from c_s^2 .

B. Modified equation of state

To further test the agreement between the observable b_{UC} and c_s^2 , we repeated the same procedure as earlier, but this time modifying the equation of state. For our modified equation of state, the hadronic part with $T \leq 150$ MeV is left unmodified, while for $T > 150$ MeV, the

³ We note that in Ref. [20] $P/\varepsilon = c_s^2$

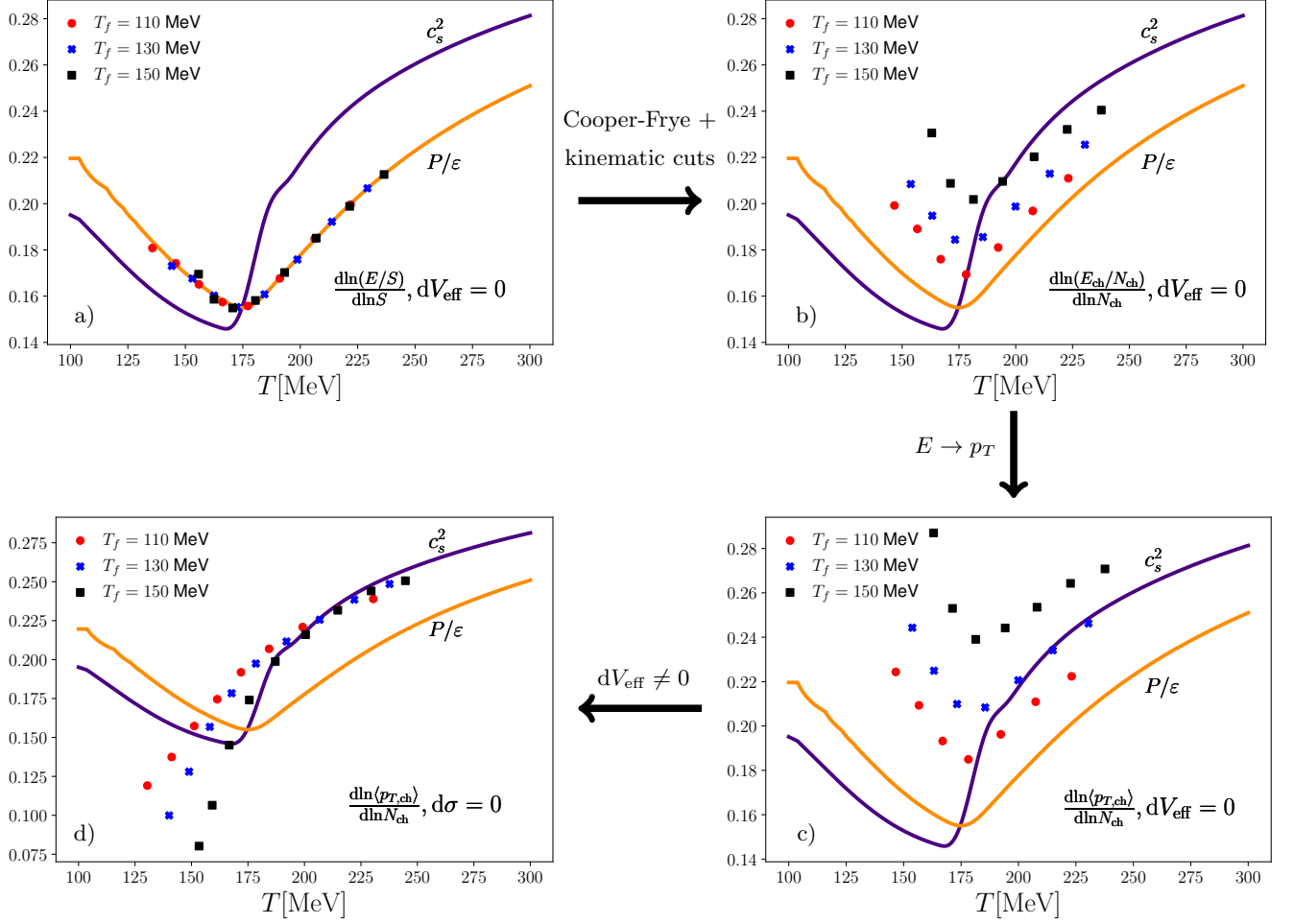


FIG. 2. Accumulation of effects that appears to coincidentally lead from P/ϵ to c_s^2 for temperatures between 200 and 250 MeV. Panel a) Assuming V_{eff} constant, the derivative $d\ln(E/S)/d\ln S$ computed from the energy E and entropy S on constant-temperature hypersurfaces leads to P/ϵ , and not c_s^2 . Panel b) When we replace the hydrodynamic energy on the hypersurface with the Cooper-Frye particle energy with midrapidity cuts, a first error is generated, which scatters the point above P/ϵ . Panel c) When we replace the mean energy E/S with $\langle p_T \rangle$, the points are scattered even more randomly above P/ϵ . Panel d) When we finally relax the assumption that $V_{\text{eff}} = \text{const}$ (which was a central ingredient in the original derivation by [11, 12]), and fix instead the width σ of the initial profile, the points rearrange on a curve that happens to fall on top of the c_s^2 -curve between temperatures 200 and 250 MeV.

speed of sound is given by

$$c_s^2(T) = c_{s,\text{QCD}}^2(T) \left[1 + 35 \tanh\left(\frac{T - T_a}{\text{GeV}}\right) e^{-\frac{(T - T_a)^2}{\delta T^2}} \right], \quad (11)$$

where $T_a = 220$ MeV, and $\delta T = 20$ MeV and $c_{s,\text{QCD}}^2$ is the speed of sound from the QCD equation of state used earlier. Other thermodynamic quantities above temperature 150 MeV are then constructed from $c_s^2(T)$ in such a way that all thermodynamic identities are satisfied. While using the modified equation of state, the initial state parameters were varied between values $[0.23, 0.67]$, $[0.8, 0.96]$ GeV for T_0 , and $[4.38, 5.06]$ fm for σ .

In Fig. 3, we show the same set of plots as discussed in the previous subsection, but this time with our mod-

ified equation of state. When $dV_{\text{eff}} = 0$ our previous observations hold. Firstly, for $d\ln(E/S)/d\ln S$ in Fig. 3a), the points agree with P/ϵ , regardless of the hypersurface temperature T_f . Secondly, when computing $d\ln\langle(E_{\text{ch}}/N_{\text{ch}})\rangle/d\ln N_{\text{ch}}$ (Fig. 3b)), each set of points for a given T_f display a pattern similar to P/ϵ , with lower T_f having better quantitative agreement. Thirdly, the mass corrections due to using transverse momentum instead of energy lead to slight behavior changes in Fig. 3c) with respect to Fig. 3b). However, in Fig. 3d) when computing the exponent b_{UC} by only varying the normalization of initial conditions (changing T_0 but keeping σ fixed in Eq. (8)), we no longer see a correlation between b_{UC} and c_s^2 in the 180-230 MeV temperature range. For the very high temperatures b_{UC} again approaches c_s^2 . From

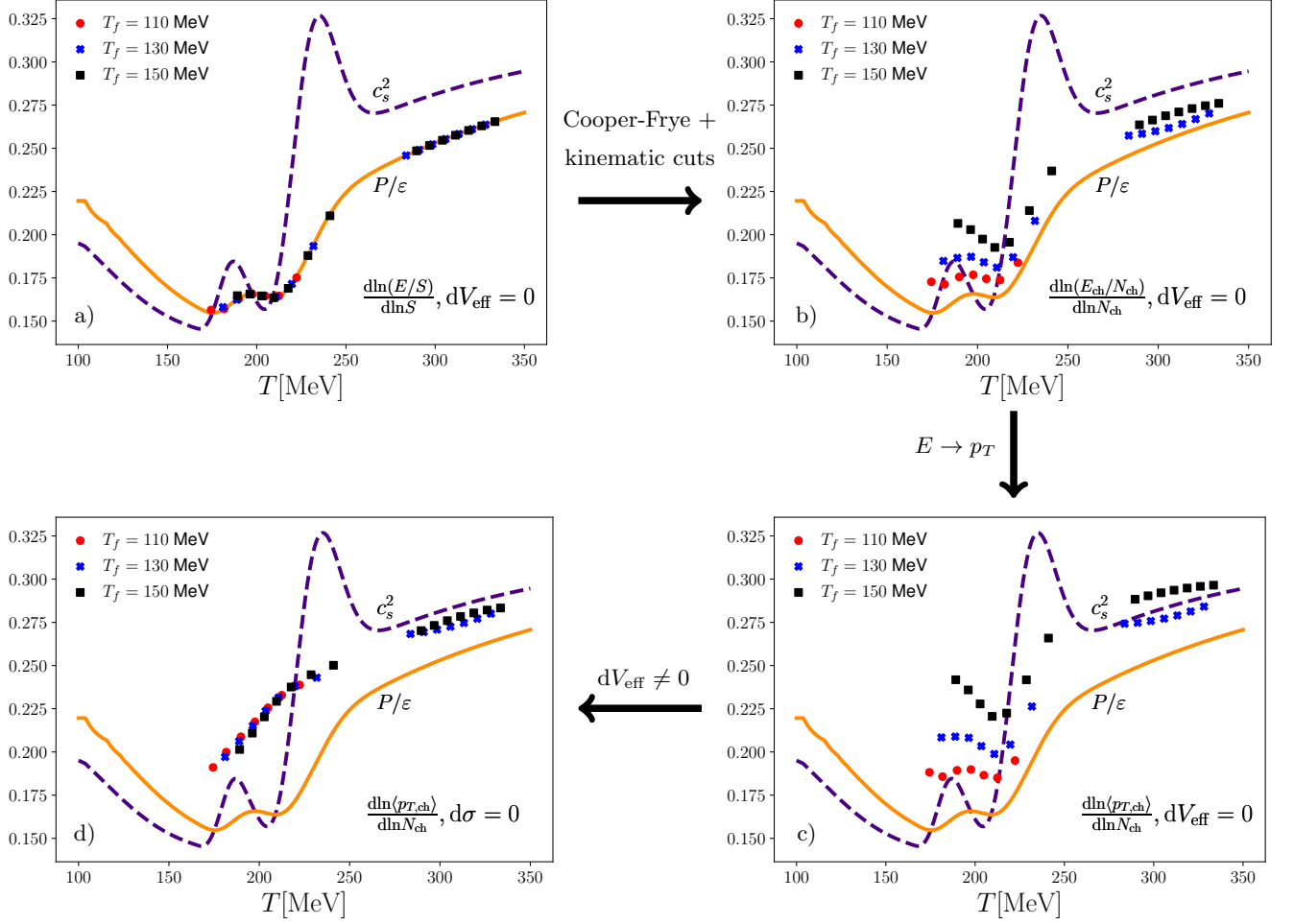


FIG. 3. Same as Fig 2 but with a modified equation of state for temperatures $T > 150$ MeV, see Eq. (11). The systematics for panels a), b) and c) are comparable to those seen earlier, while observable b_{UC} in panel d) shows much larger deviations from the speed of sound c_s^2 .

Figs. 3 and 4, it appears that b_{UC} tracks c_s^2 more closely at high effective temperatures where c_s^2 is varying slowly. It is not clear if this is related to these high T_{eff} regions being closer to the conformal ($c_s^2 = 1/3$) limit, or to high T_{eff} systems being longer lived, two effects studied in Ref. [20]. The significant effect of enforcing a constant effective volume — panels (c) and (d) — seems to preclude a simple explanation.

C. The relation between $\langle p_T \rangle$ and T_{eff}

We also studied the validity of assumption $\langle p_T \rangle \propto T_{eff}$. In Fig. 4, we show $\langle p_T \rangle / T_{eff}$ as a function of charged particle multiplicity for the QCD equation of state (left panel) and the modified equation of state (right panel, see Eq. (11)). We notice that the ratio $\langle p_T \rangle / T_{eff}$ has a clear dependence on the temperature of the hypersurface in both cases. Besides, in the left panel of Fig. 4, we see that for sufficiently large multiplicities, the range of

values of $\langle p_T \rangle / T_{eff}$ lies within a horizontal band whose width depends non-trivially on the hypersurface temperature. We see that these bands lie around $\langle p_T \rangle / T_{eff} \approx 3.2$ for $T_f = 150$ MeV, $\langle p_T \rangle / T_{eff} \approx 3.5$ for $T_f = 130$ MeV, and $\langle p_T \rangle / T_{eff} \approx 3.8$ for $T_f = 110$ MeV, thus the estimate that $\langle p_T \rangle / T_{eff} \approx 3.0$ [11] is not general. For $dN/d\eta \lesssim 500$, the band is such that $\langle p_T \rangle / T_{eff}$ is not approximately constant, but rather decreases as the multiplicity decreases. The effect of hypersurface temperature and multiplicity dependence on $\langle p_T \rangle / T_{eff}$ has also been seen in Refs. [11, 13].

With the modified equation of state (Eq. (11)), in the right panel of Fig. 4, the shape of the bands changes significantly: they become wider at high multiplicities and possess a different range in multiplicity even though the range of values of T_0 and σ are very similar (see, respectively, text below Eq. (8) and text below Eq. (11)). Also in this case, $\langle p_T \rangle / T_{eff} \approx 3.0$ is also not accurate.

We emphasize that even in the situations where $\langle p_T \rangle / T_{eff}$ ratio seems to be almost a constant, it does

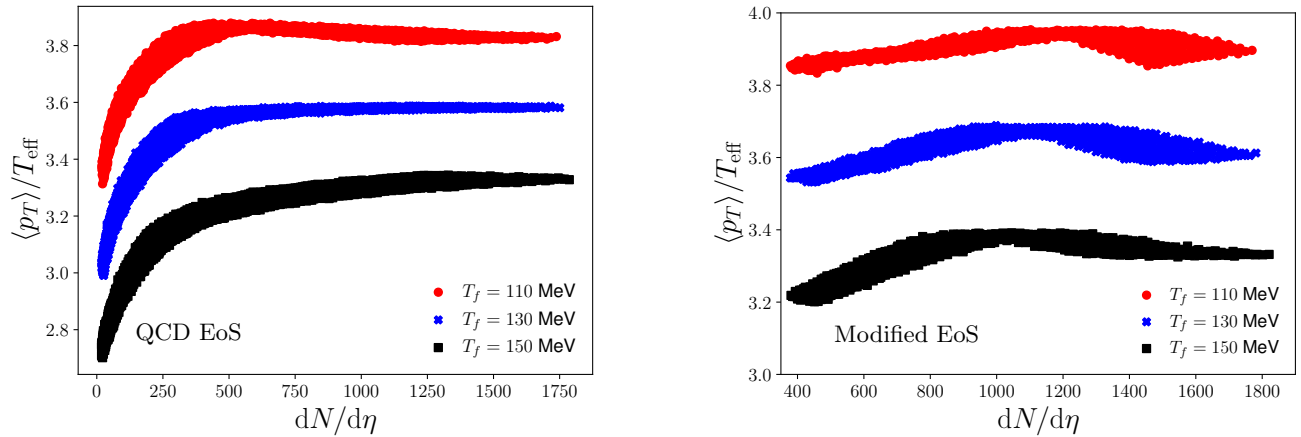


FIG. 4. The $\langle p_T \rangle / T_{\text{eff}}$ ratio as a function of charged hadron multiplicity for QCD equation of state (left-hand panel) and the modified equation of state (right-hand panel).

not guarantee that the observable b_{UC} would be c_s^2 even when $dV_{\text{eff}} = 0$ (see Fig. 2c)). The reason for this is the following. It is possible to write

$$b_{\text{UC}} = d \ln T_{\text{eff}} / d \ln N + d \ln (\langle p_T \rangle / T_{\text{eff}}) / d \ln N, \quad (12)$$

where the first term is c_s^2 , if $N \propto S$ and $dV_{\text{eff}} = 0$. When the $\langle p_T \rangle / T_{\text{eff}}$ ratio is exactly constant, the second term would be zero and c_s^2 is recovered. However, since the $\langle p_T \rangle / T_{\text{eff}}$ forms a finite band even at high multiplicities, its derivative can get slightly different values depending on what is the underlying variation that causes the changes in the multiplicity and mean transverse momentum. It turns out that when we choose a variation for which $dV_{\text{eff}} = 0$, then $d \ln (\langle p_T \rangle / T_{\text{eff}}) / d \ln N$ term modifies the functional form of b_{UC} significantly.

V. DISCUSSION

Heavy-ion collisions are evidently not simple thermodynamic systems, and the hypersurface energy E and entropy S are not experimentally measurable. What is measured is typically the mean transverse momentum $\langle p_{T,\text{ch}} \rangle$ and the multiplicity of charged hadrons N_{ch} in a specific range of pseudorapidity. In ultracentral collisions, these are found to be related by $\langle p_{T,\text{ch}} \rangle \propto N_{\text{ch}}^{b_{\text{UC}}}$ with b_{UC} a number in the vicinity of $1/4$. The observable b_{UC} has been previously assumed to be so closely related to the speed of sound as to provide constraints on the equation of state of QCD that are competitive with lattice QCD [14]. As discussed in this work, this interpretation of b_{UC} is not supported by closer scrutiny. Under specific conditions ($N \propto S$, $\langle p_T \rangle \propto E/S$, no rapidity cut, and $dV_{\text{eff}} = 0$), the exponent b_{UC} should be measuring the ratio of the pressure and the energy density P/ε at the effective temperature T_{eff} defined by Eq.(2). As seen in Figure 2, we found evidence that this is not possible in reality.

On the other hand, under other conditions, b_{UC} does appear to match the speed of sound — the original interpretation for b_{UC} . Specifically, if the condition $dV_{\text{eff}} = 0$ is relaxed such that the variations of $\langle p_T \rangle$ and N arise purely from the normalization of initial temperature T_0 , the result from numerical simulations for b_{UC} is *sometimes* rather close to the speed of sound (Figs. 2(d) and 3(d)). This is consistent with results from other groups' numerical simulations [11, 13], where $dV_{\text{eff}} = 0$ was also *not* enforced.

However, our results indicate that the agreement of b_{UC} with the speed of sound in Figs. 2(d) and 3(d) is not a general result, for multiple reasons:

- b_{UC} and c_s^2 only agree in certain ranges of temperature, and large deviations appear at low temperature (Figure 2(d)),
- b_{UC} and c_s^2 only agree if the condition $dV_{\text{eff}} = 0$ is relaxed (Figure 2(d) vs Figure 2(c)), while theoretical arguments for this relation rely on the condition $dV_{\text{eff}} = 0$,
- If the equation of state is modified, much larger deviations between b_{UC} and c_s^2 can be observed, as shown in Figure 3.

We believe that these three observations confirm that $c_s^2(T_{\text{eff}})$ cannot be equated to b_{UC} in general. In fact, it appears that the only way to know if b_{UC} accurately tracks the speed of sound is to have verified that relation ahead of time with numerical simulations that use the lattice equation of state. We emphasize that the tests above ignore other expected challenges, such as the effect of viscosity, p_T cuts, etc. discussed in other publications [18, 21].

Additional insights from numerical simulations can help find less direct but more accurate relations between b_{UC} and the equation of state, as explored in Refs. [21, 22]

for example. It is our understanding that b_{UC} was never an independent measurement of the speed of sound, since (i) the relation between $\langle p_T \rangle$ and T_{eff} was evaluated using the lattice equation of state of QCD, and (ii) it does not appear possible to know ahead of time if b_{UC} and the speed of sound will agree without numerical simulations that use the lattice equation of state. Hence, we believe that adding more information from numerical simulations (e.g. volume variation corrections) to obtain a more complex relation between b_{UC} and QCD thermodynamic quantities is consistent with the original approach. Direct comparison of numerical simulations to multiplicity and average transverse momentum data from ultra-central collisions is evidently also an effective approach to leverage the thermodynamic information available in these collisions.

In summary, from numerical simulations and experimental data, it appears to be generally true that $\langle p_{T,\text{ch}} \rangle \propto N_{\text{ch}}^{b_{\text{UC}}}$ and that the values of b_{UC} extracted — broadly between 0.15 and 0.3 — are in the range expected for the speed of sound of QCD or the ratio P/ε of the pressure over the energy density. The prediction [11]

that the exponent b_{UC} should be numerically similar to the speed of sound of QCD is clearly a success of our understanding of relativistic heavy-ion collisions. However, turning this argument around and promoting b_{UC} as a systematic measurement of the speed of sound is a completely different matter that is not supported by our study.

Acknowledgments

The authors thank Fernando Gardim, Wei Li, Andi Mankolli, Jean-Yves Ollitrault, Shengquan Tuo, Julia Velkovska and Li Yan for useful discussions. H.H., J.-F. P., M. S. and G. S. R. are supported by Vanderbilt University and by the U.S. Department of Energy, Office of Science under Award Number DE-SC-0024347. H.H. is also partly supported by the U.S. Department of Energy, Office of Science under Award Number DE-SC0024711, and the National Science Foundation under Grant No. DMS-2406870. L.G. is partially supported by a Vanderbilt Seeding Success grant.

-
- [1] C. Y. Wong, *Introduction to high-energy heavy ion collisions* (1995).
 - [2] K. Yagi, T. Hatsuda, and Y. Miake, *Quark-gluon plasma: From big bang to little bang*, Vol. 23 (2005).
 - [3] R. Vogt, *Ultrarelativistic heavy-ion collisions* (Elsevier, Amsterdam, 2007).
 - [4] U. Heinz and R. Snellings, *Ann. Rev. Nucl. Part. Sci.* **63**, 123 (2013), [arXiv:1301.2826 \[nucl-th\]](#).
 - [5] U. Heinz and B. Schenke (2024) [arXiv:2412.19393 \[nucl-th\]](#).
 - [6] S. Borsanyi, G. Endrodi, Z. Fodor, A. Jakovac, S. D. Katz, S. Krieg, C. Ratti, and K. K. Szabo, *JHEP* **11**, 077 (2010), [arXiv:1007.2580 \[hep-lat\]](#).
 - [7] A. Bazavov *et al.*, *Phys. Rev. D* **80**, 014504 (2009), [arXiv:0903.4379 \[hep-lat\]](#).
 - [8] S. Borsanyi, Z. Fodor, J. N. Guenther, R. Kara, S. D. Katz, P. Parotto, A. Pásztor, C. Ratti, and K. K. Szabó, *Phys. Rev. Lett.* **126**, 232001 (2021), [arXiv:2102.06660 \[hep-lat\]](#).
 - [9] A. Bazavov *et al.*, *Phys. Rev. D* **95**, 054504 (2017), [arXiv:1701.04325 \[hep-lat\]](#).
 - [10] S. Pratt, E. Sangaline, P. Sorensen, and H. Wang, *Phys. Rev. Lett.* **114**, 202301 (2015), [arXiv:1501.04042 \[nucl-th\]](#).
 - [11] F. G. Gardim, G. Giacalone, M. Luzum, and J.-Y. Ollitrault, *Nature Phys.* **16**, 615 (2020), [arXiv:1908.09728 \[nucl-th\]](#).
 - [12] F. G. Gardim, G. Giacalone, and J.-Y. Ollitrault, *Phys. Lett. B* **809**, 135749 (2020), [arXiv:1909.11609 \[nucl-th\]](#).
 - [13] F. G. Gardim, A. V. Giannini, and J.-Y. Ollitrault, *Phys. Lett. B* **856**, 138937 (2024), [arXiv:2403.06052 \[nucl-th\]](#).
 - [14] A. Hayrapetyan *et al.* (CMS), *Rept. Prog. Phys.* **87**, 077801 (2024), [arXiv:2401.06896 \[nucl-ex\]](#).
 - [15] G. Aad *et al.* (ATLAS), *Phys. Rev. Lett.* **133**, 252301 (2024), [arXiv:2407.06413 \[nucl-ex\]](#).
 - [16] O. V. Rueda (ALICE), *PoS ICHEP2024*, 600 (2025), [arXiv:2409.20470 \[nucl-ex\]](#).
 - [17] A. Bazavov *et al.* (HotQCD), *Phys. Rev. D* **90**, 094503 (2014), [arXiv:1407.6387 \[hep-lat\]](#).
 - [18] G. Nijss and W. van der Schee, *Phys. Lett. B* **853**, 138636 (2024), [arXiv:2312.04623 \[nucl-th\]](#).
 - [19] L. Van Hove, *Phys. Lett. B* **118**, 138 (1982).
 - [20] G. Soares Rocha, L. Gavassino, M. Singh, and J.-F. Paquet, *Phys. Rev. C* **110**, 034913 (2024), [arXiv:2405.10401 \[hep-ph\]](#).
 - [21] Y.-S. Mu, J.-A. Sun, L. Yan, and X.-G. Huang, (2025), [arXiv:2501.02777 \[nucl-th\]](#).
 - [22] J.-A. Sun and L. Yan, *Phys. Lett. B* **866**, 139507 (2025), [arXiv:2407.05570 \[nucl-th\]](#).
 - [23] P. Huovinen and H. Petersen, *Eur. Phys. J. A* **48**, 171 (2012), [arXiv:1206.3371 \[nucl-th\]](#).
 - [24] B. Schenke, S. Jeon, and C. Gale, *Phys. Rev. C* **82**, 014903 (2010), [arXiv:1004.1408 \[hep-ph\]](#).
 - [25] S. Ryu, J. F. Paquet, C. Shen, G. S. Denicol, B. Schenke, S. Jeon, and C. Gale, *Phys. Rev. Lett.* **115**, 132301 (2015), [arXiv:1502.01675 \[nucl-th\]](#).
 - [26] J.-F. Paquet, C. Shen, G. S. Denicol, M. Luzum, B. Schenke, S. Jeon, and C. Gale, *Phys. Rev. C* **93**, 044906 (2016), [arXiv:1509.06738 \[hep-ph\]](#).
 - [27] S. Ryu, J.-F. Paquet, C. Shen, G. Denicol, B. Schenke, S. Jeon, and C. Gale, *Phys. Rev. C* **97**, 034910 (2018), [arXiv:1704.04216 \[nucl-th\]](#).
 - [28] F. Cooper and G. Frye, *Phys. Rev. D* **10**, 186 (1974).
 - [29] F. Cooper, G. Frye, and E. Schonberg, *Phys. Rev. D* **11**, 192 (1975).
 - [30] C. Shen, Z. Qiu, H. Song, J. Bernhard, S. Bass, and U. Heinz, *Comput. Phys. Commun.* **199**, 61 (2016), [arXiv:1409.8164 \[nucl-th\]](#).